Engineering Structures 31 (2009) 2954–2965

Contents lists available at ScienceDirect

Engineering Structures

journal homepage: www.elsevier.com/locate/engstruct

Longterm sensor-based monitoring of an LRFD designed steel girder bridge

Samir N. Shoukry [a], Mourad Y. Riad [b,*], Gergis W. William [b]

[a] Department of Mechanical and Aerospace Eng., West Virginia University, PO Box 6106, Morgantown, WV 26506, USA
[b] Department of Civil and Environmental Eng., West Virginia University, PO Box 6103, Morgantown, WV 26506, USA

ARTICLE INFO

Article history:
Received 2 December 2008
Received in revised form
20 July 2009
Accepted 20 July 2009
Available online 4 August 2009

Keywords:
Long-term monitoring
Instrumentation
Steel girder bridge
End-bearing movement
Bridge temperature gradients
Environmental loading

ABSTRACT

The new AASHTO LRFD bridge design specifications allow the use of the arching action mechanism in concrete slabs to design lightweight bridge decks. The Star City Bridge in Morgantown, WV is designed according to the LRFD code and measures 306 m over 4 spans. In an effort to demonstrate the long-term performance of in-service light-weight bridge decks, the bridge was heavily instrumented with over 700 sensors that record the response of main superstructure elements to various loading parameters. Data are being recorded every 20 min and provide continuous monitoring and evaluation of the performance of the bridge since construction in 2003–2004. This paper describes the instrumentation system installed on the Star City Bridge and demonstrates the performance of the steel superstructure over 4 years from the time of deck pouring. The expansion and contraction of the superstructure at one end contributed to the relief of environmentally induced internal stresses in the longitudinal direction. Bearing movement constrains on the other end introduced normal forces in the steel girders that are not taken into consideration in deck designs. Straining action variations due to environmental loading amounted to 20% of their initial values after pouring the deck. Temperature data shows development of a non-linear gradient across the bridge width, which explains an additional build-up of stresses found on diaphragm members at the outside girders. Compared to the LRFD specifications, the measured maximum positive temperature gradient across the bridge superstructure was found to have close values, while the maximum negative temperature gradient recorded a higher profile.

1. Introduction

According to the ASCE report card, as of December 2008, 12.1% of bridges were categorized as structurally deficient and 14.8% were categorized as functionally obsolete. AASHTO estimated in 2008 that about $ 48 billion are needed to repair structurally deficient bridges and that $ 91 billion are estimated to improve functionally obsolete bridges [1]. Repair of bridges is costly and often troublesome because of compulsory traffic flow disruptions that become an overburden on motorists and commuters. Because of safety concerns, inspections of existing bridges are being conducted routinely following the National Bridge Inspection Program [2]. Those inspections provide a record of the bridges' conditions and are often used to establish priorities for repair and rehabilitation actions and to perform life-cycle management on highway bridges [3,4]. However, visual inspections of bridges have multiple limitations. Inspectors have access to very limited testing tools on site and have to rely on their experience and personal judgment to identify and classify signs of deteriorations. Visual inspections are time consuming and embody a financial overburden that state highway agencies are overtaking. Meanwhile, more efforts are being conducted to develop remote sensing systems that would allow more sophisticated and accurate methods to assess the structural performance of bridge elements and, hence, provide a rational method of making decisions about the condition of particular bridges. A laboratory study to develop a comprehensive small scale instrumentation system for bridge monitoring demonstrated that reliable and feasible bridge monitoring systems was achievable [5]. Implementations of sensor-based health monitoring systems on existing bridges demonstrated the ability of such systems to render valuable data [6–13]. The use of dynamic techniques to evaluate bridge damage in the field proved to be useful tools. De Wolf et al. [14] used traffic loads as excitation to monitor a two-span highway bridge. A similar approach to use ambient loading was followed by Nagayama et al. [15] to identify modal properties of the Hakucho Bridge in Japan. A study by Ren et al. [16] was conducted on the John A. Roebling Suspension Bridge over the Ohio River to determine the live load response and safety margins of the bridges' main cables. Raghavendrachar and Aktan [17], Aktan et al. [18], Toksoy Aktan [19] and Alampalli et al. [20] used impact testing techniques for bridge monitoring and damage detection. One major challenge that faces applications of damage identification using vibration analyses of infrastructures is that environmental variations including temperature and moisture changes affect

* Corresponding author. Tel.: +1 3042933031; fax: +1 3042937109.
E-mail address: myriad@mail.wvu.edu (M.Y. Riad).

0141-0296/$ – see front matter © 2009 Elsevier Ltd. All rights reserved.
doi:10.1016/j.engstruct.2009.07.023

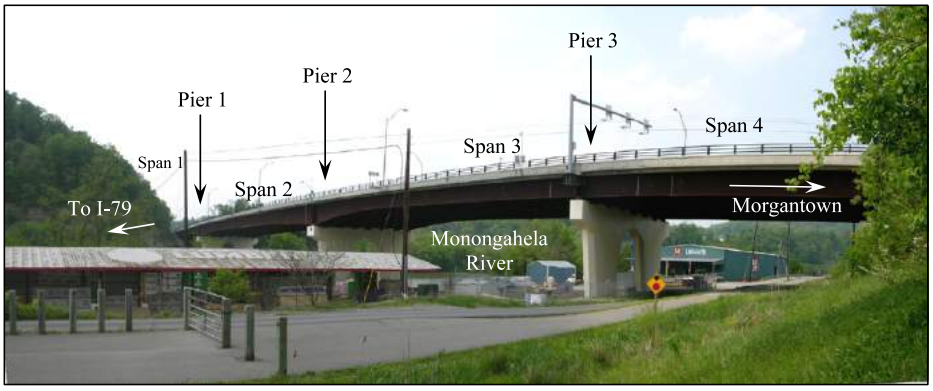

Fig. 1. Star City Bridge near Morgantown, WV.

the dynamic response of such structures and cannot be overlooked. Sohn et al. [21] indicated that the measured natural frequency of the Alamosa Canyon Bridge in New Mexico varied by 5% during just a 24 h test period.

In 2003–2004 the authors implemented an intensive long term remote monitoring study on the Star City Bridge in Morgantown, WV. The sensing system is able to provide uninterrupted data that can be transmitted to any place through a phone line. The data provide information on the performance of various bridge elements at any given moment, which permits engineers to monitor the behavior of the bridge superstructure and analyze its response to traffic loads as well as environmental changes. The sensory system provides a database consisting of key-performance parameters that evaluate the bridge long-term performance such as the tri-axial state of stress and strains in the concrete deck, bending moments as well as shearing stresses and inclinations of the steel girders, forces at the diaphragm members, expansion and contraction of bridge ends, strains and stresses in rebars, crack formation in the concrete deck, along with temperature profiles along the deck. Furthermore, a Weigh in Motion device is installed at the bridge entrance and provides continuous data of the traffic crossing the bridge. The recorded data along 4 years since pouring the deck offer insight into the behavior of lightweight bridge decks.

The Star City Bridge is designed according to the LRFD specifications which allows the use of high-performance materials and lightweight structures. As of October 2007, the LRFD specifications were mandated by FHWA for all state projects using federal funding. As of 2010, this design code will apply to all state bridges regardless of funding, and to local bridges using federal funding. The data collected from the Star City Bridge offers a unique opportunity to demonstrate the long term behavior of such structures designed and constructed following the LRFD code.

2. Description of the star city bridge

The new five-lane Star City Bridge is replacing a two-lane steel bridge that became a bottleneck for the flow of traffic in the Area of Morgantown, WV and its surroundings. The deck design follows the empirical design method for lightweight bridge decks which offers a remarkable amount of flexibility despite its long span [22–24]. The bridge measures 306 m in total length and consists of 5 traffic lanes that cross the Monongahela River over 4 spans to connect Star City and Morgantown (WV) to I-79. Fig. 1 is a view of the bridge after completion of construction work. The deck is composed of a reinforced concrete slab 16.5 cm thick (6.5 in.) supported by steel girders with variable inertia spaced at 3.65 meters (12 ft) and overlaid by a 5 cm (2 in.) layer of latex modified concrete. According to the design of steel girders, a variable web height was used ranging from 1.98 m (6.5 ft) to 3.96 m (13 ft). Stay-in-place forms have been used for casting the deck which followed a sequence of construction in 2 stages. Stage one consisted of casting the substructure and superstructure for the northbound portion of the bridge while maintaining traffic on the existing old bridge. Stage two consisted of the substructure and superstructure of the southbound portion of the bridge. A closure pour linked the two stages and formed the median curb. Fig. 2 illustrates a cross section of the bridge and shows the construction stages.

3. Sensory system

The sensory system is designed to provide data from both response parameters, as well as dynamic and static loading parameters. Response parameters refer to the tri-axial state of strains in the concrete deck, strains and bending moments as well as shearing stresses and inclinations of the steel girders, forces at the diaphragm members, expansion and contraction of bridge ends, strains and stresses in rebars, crack formation in concrete deck and inclinations of abutments and piers. *Strain measurements are post-processed to calculate stresses in the concrete deck, bending moments and shearing stresses in the steel girders, axial forces in the diaphragm members, and stresses in the reinforcing rebars.* Loading parameters include long term effects such as seasonal and diurnal climatic changes, and dynamic effects such as traffic loads. Figs. 3–5 illustrate various types of sensors and their locations on the bridge.

Long term response measurements are recorded using a variety of sensors *manufactured by Geokon Inc.* based on vibrating wire technology. 105 embedment strain gages *model VCE-4204* measure the tri-axial state of strain in the concrete deck. Those are placed in a strain tree configuration, as indicated in Fig. 3. The total number of strain trees is 21, and each contains 5 strain gages as well as 2 sister bars *model 4911*. 42 sister bars continuously record forces in reinforcing steel rebars. 56 embedment crack meters *model 4430* record the initiation and propagation of any concrete transverse cracks. Those are placed in series of 4 sensors at 14 locations along the deck. 2 displacement transducers (Convergence meters) *model 4425* record the overall expansion and contraction of the bridge ends relative to both abutments due to seasonal and daily temperature changes, as shown in Fig. 4. A special fixture was manufactured to house those 2 sensors and adopt them to be embedded in concrete. Each vibrating wire sensor is equipped with a thermistor *model YSI 44005* that provides continuous records of the temperature in the medium surrounding the sensor. The temperature measurement is used to apply temperature compensation to correct the variation between the coefficient of thermal expansion of the sensor material and that of the measured medium. There are 439 thermistors involved in this instrumentation system that provide an overall thermal map of the concrete deck temperature and record temperature data for the sensors thermal compensation. 200 strain gages *model VSM 4000* are installed on the steel girders to record both

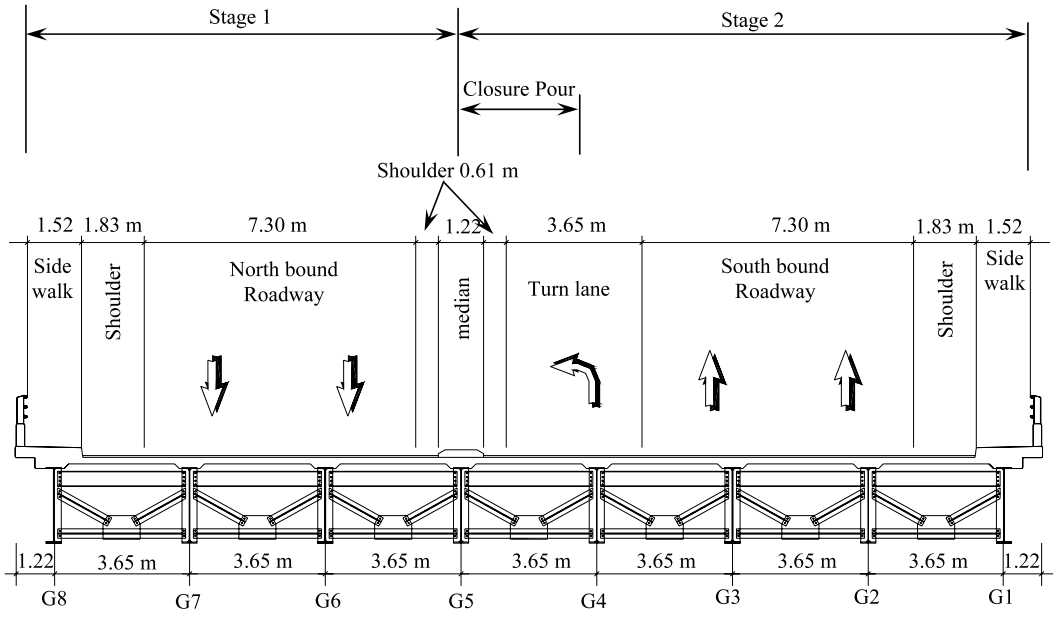

Fig. 2. Bridge cross section and sequence of construction.

Table 1
Specifications of long-term response sensors.

Sensor model No.	Description	Number employed	Nominal range	Resolution	Frequency range	
					Start (Hz)	End (Hz)
VCE-4204	Embedment strain gage	105	3000 $\mu\varepsilon$	1 $\mu\varepsilon$	800	1600
4911	Sister bar	42	2500 $\mu\varepsilon$	0.4 $\mu\varepsilon$	1800	2800
4430	deformation meter	56	25 mm	0.00625 mm	1200	2800
YSI 44005	thermistor	405	200 °C	0.5 °C	–	–
4425	Displacement transducer	2	30 cm	0.075 mm	1200	2800
VSM4000	Weldable strain gage	200	3000 $\mu\varepsilon$	0.1 $\mu\varepsilon$	400	1000

shear and bending *strains* as well as straining actions in the diaphragm members. Mounting those particular sensors on the steel girders represented a challenge, since any type of welding was not allowed by the WVDOT due to concerns of excessive stress concentrations resulting from localized heat generation during the welding process. A bonding technique was adopted for bonding the selected strain gages to the steel girders and proved to be very efficient. *The mounting blocks as well as the receiving surface on the steel girders are grinded and cleaned with acetone in order to increase surface friction and to remove all scales, debris and rust before receiving the bonding agent. An epoxy bonding material (Loctite H4500) is applied on the steel member at the location of the sensor that is pre-marked. The sensor is mounted on the surface and kept in position by a pair of magnets that were positioned on the mounting blocks. After the bonding agent is set (3 min), the bonded sensor and blocks are covered with a plastic sheet and sealed with duck tape to protect from rain or moisture. The location of each sensor is revisited where the coil assembly and cable are attached to the sensor, the mid-range is set, and a layer of rubber moisture sealant is spread on the exposed bonding agent for protecting against moisture.* 14 innovative vibrating wire embedment strain gages record the dynamic stresses in 2 directions in the concrete deck along the wheel paths due to moving traffic. Table 1 *lists the installed vibrating wire sensors along with main characteristics of each model*

Angles of inclination of the steel girders at 4 locations, as well as abutment 2 and pier 3, are being monitored through inclinometers. Inclinometers' data are being transmitted wirelessly through an in-house built digital wireless system to the field office. *Wireless sensing systems emerged as a solution to cost prohibitive and tedious tasks that require drawing extensive cable lengths into far reaching elements in large structures. Pioneering in this field,* Maser et al. [25] *deployed a wireless sensor network on a highway bridge where a wireless transceiver used one-hop communication with a base station that was interconnected using cellular telephony. Straser and Kiremidjian* [26] *suggested the use of radio modules with sensors for structural monitoring purposes. Their wireless sensing unit consisted of a low-power 8-bit microcontroller that converted the analog output signal from sensors into a digital high resolution format.* Bennett etal [27] *embedded a wireless sensing unit in a flexible highway pavement to record temperature and strain measurements.* Lynch [28] *integrated sophisticated dual core microcontrollers with wireless sensors for the execution of embedded engineering algorithms.* Lynch [29] *continued this effort by integrating a four-channel 12-bit digital-to-analog converter (DAC) that was employed to conduct a study of wireless piezoelectric pads mounted to the surface of structural plates for damage detection.* Mitchell et al. [30] *proposed a two-tier Web-controlled wireless network sensors for structural health monitoring.* Kottopalli et al. [31] *suggested also a two-tiered wireless sensor network architecture to overcome time synchronization problems as well as challenges with data transmission rates and power efficiency. Later,* Mastroleon et al. [32] *improved power efficiency of the system suggested by Kottopali et al. by upgrading the original hardware components.* Lynch et al. [33] *described wireless sensing prototypes that were used to monitor the Alamosa Canyon Bridge in New Mexico as a study to investigate the concept of health monitoring of real structures using wireless sensing elements.* Aoki et al. [34] *designed a compact wireless system named Remote Intelligent Monitoring System (RIMS) for intelligent bridge and infrastructure maintenance purposes using internal 12-bit ADC microcontroller and three-axis MEMS piezo-resistance accelerometers. In recent years, various prototypes of wireless sensing devices have been developed.* Shinozuka [35] *described DuraNode*

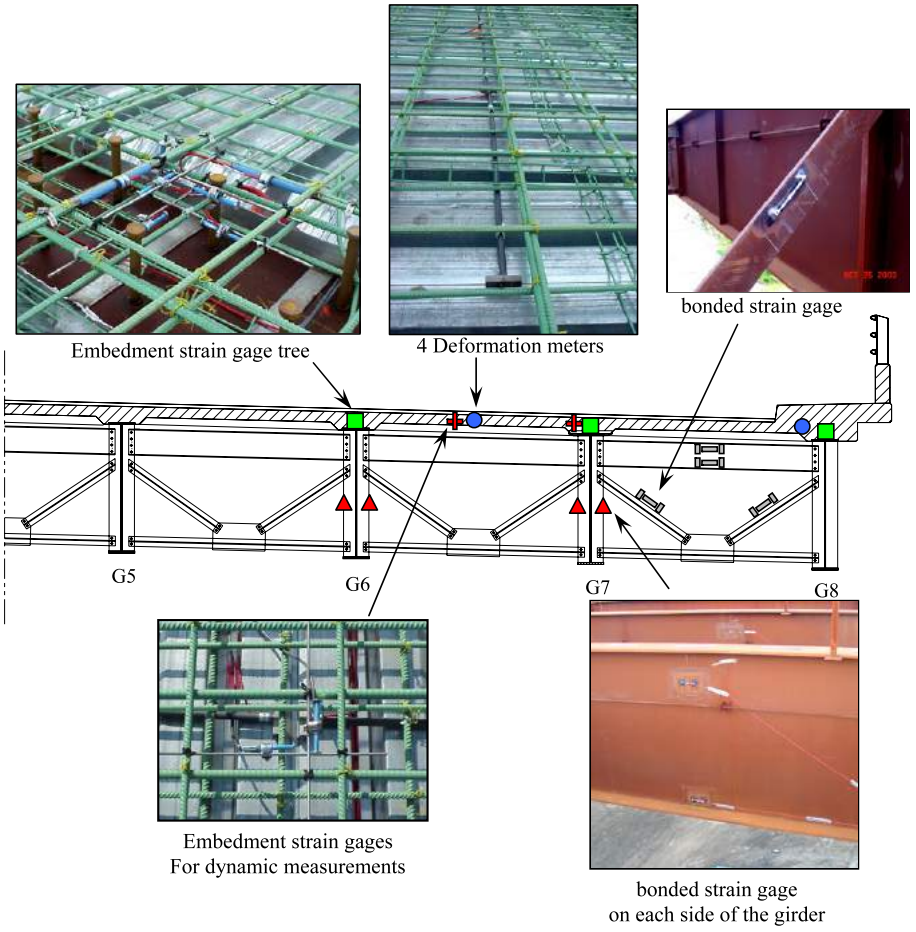

(a) Details of instrumentation at location between bridge supports.

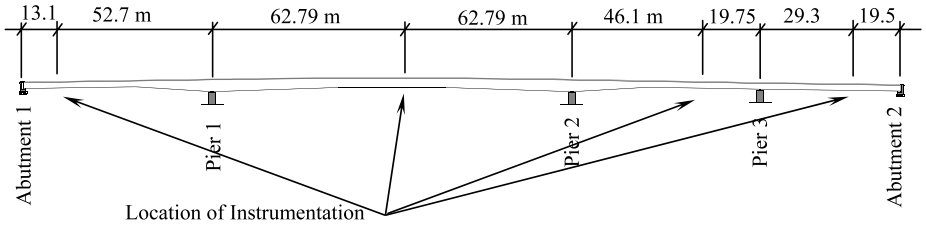

(b) Location of instrumentation between bridge supports.

Fig. 3. Typical instrumentation between bridge supports (max. +ve and/or −ve bending moment).

that contains two accelerometers for measuring vibrations in three dimensions, while Basheer et al. [36] *proposed the ISC-iBlue wireless sensor node that senses strain values and uses Bluetooth wireless radio for data transmission.* Lynch et al. [37] *monitored forced acceleration response of Geumdang Bridge in Korea through 14 wireless sensors.* Ruiz-Sandoval et al. [38] *developed a wireless sensor network based on MEMS accelerometer and strain sensor board for structural health monitoring where they used Mica motes for communication and control.* Pakzad et al. [39] *designed and developed an integrated hardware and software system for a scalable wireless sensor network for structural health monitoring.*

Given the relatively small values of the analog data and the high level of external perturbations, transferring inclinometers' data through cables hundreds of feet away from the place of origin would be highly risky. Amplifying the signal before transmission would not solve the problem, considering the risk of signal contamination with amplified noise. Therefore, the system was designed to convert the analog values produced by the inclinometers into a digitized format at the location of each inclinometer and to transmit them wirelessly. The digitized data are fed into an RF transceiver through a quarter wave antenna as an input. The RF transceiver runs in a license free range and transmits those data to the corresponding receiver which converts them into a digital format suitable for a single board computer (SBC). Using the master–slave concept, the whole process of data collection and storage is controlled through the (SBC) being the master. Fig. 4 include a picture of one inclinometer setup placed on abutment 2 and its data transmission device. Diurnal and seasonal climatic changes are important parameters that contribute to the long term loading configuration. Thus, a weather station is installed at the bridge site and provides continuous records of weather data. The weather station provides measurements of wind speed and direction, ambient temperature, relative humidity, rain fall, and solar radiation.

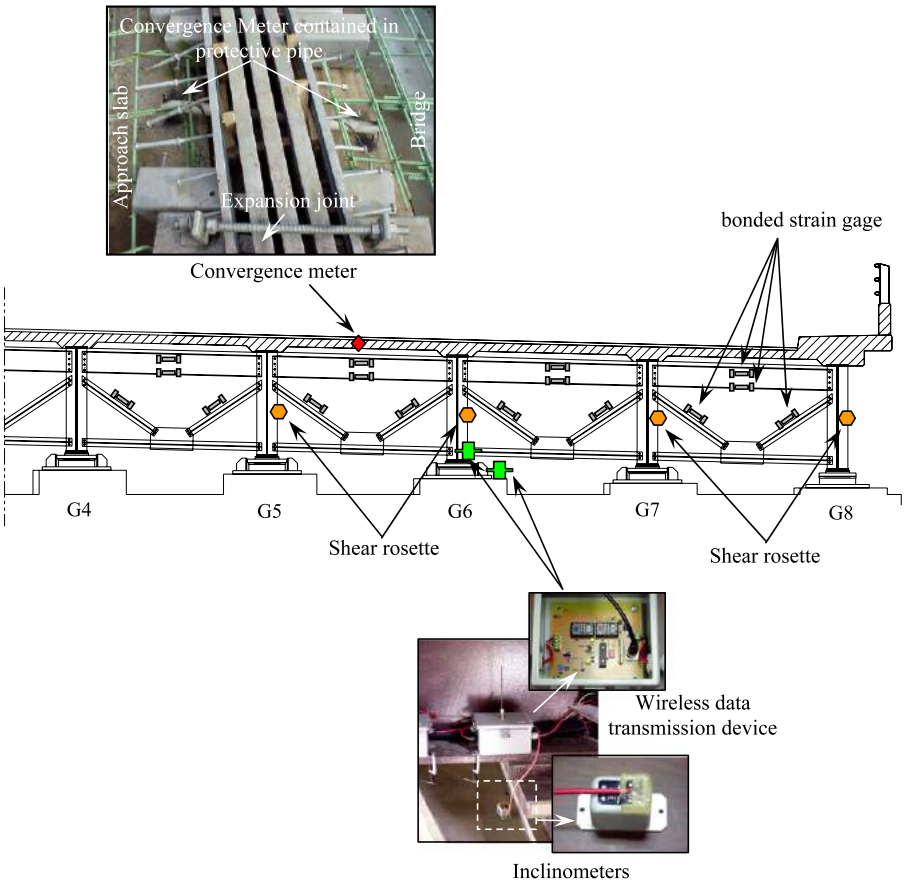

Fig. 4. Typical instrumentation at location of abutments.

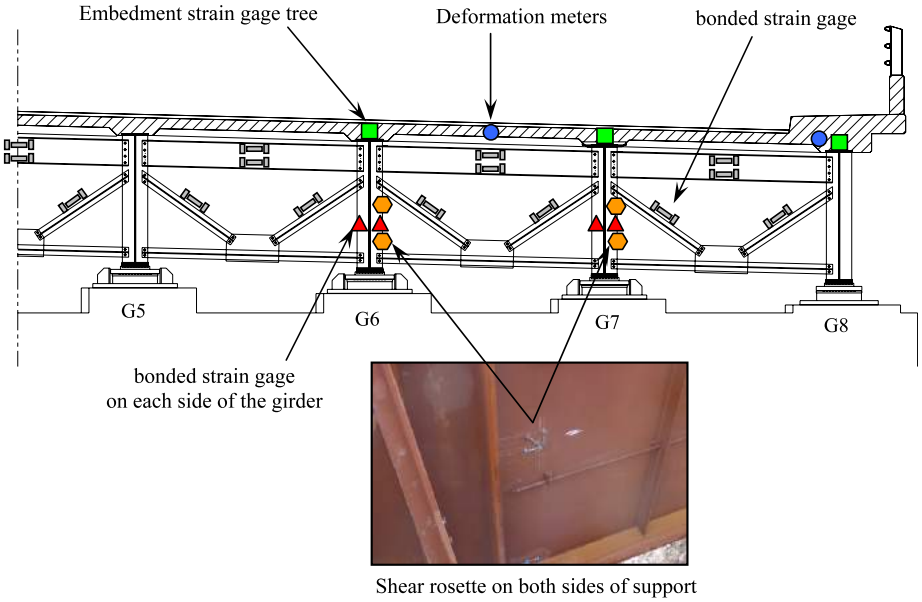

Fig. 5. Instrumentation at location of piers (max. −ve bending moment).

3.1. Measurements of traffic spectrum

Peizo-electric sensors are the core of a weigh in motion (WIM) system that is installed at the bridge entrance and provides continuous time histories of axle loads crossing the southbound roadway. The system is designed in an attempt to create a cost effective device based on commercially available components and in-house built data acquisition system as well as in-house developed software. Data output formats and protocols for equipment calibration are developed following the guidelines of ASTM-E-1318 [40]. The WIM system is installed on the driving lane of the southbound roadway which carries most of the traffic and is capable of providing data including wheel weight, actual speed, number of axles for each vehicle, and distance between axles, as vehicles travel at highway speeds. The WIM System uses two piezoelectric sensors, along with two inductive loops and loop detectors.

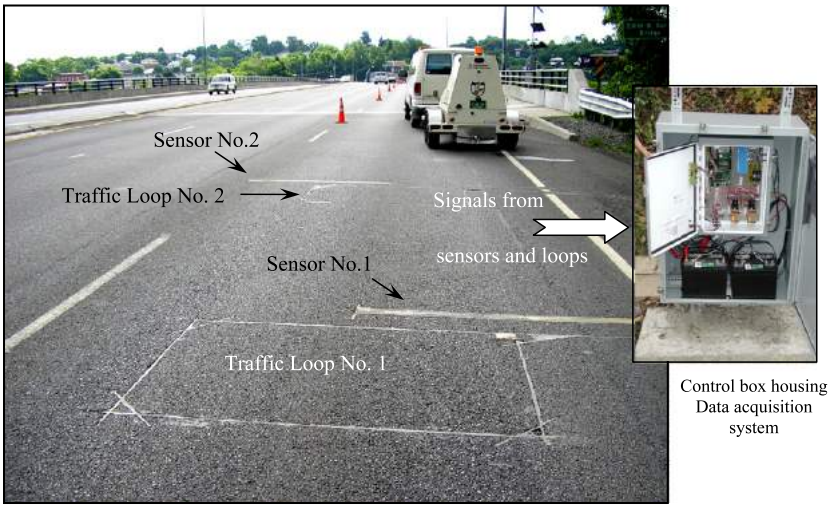

Fig. 6. Weigh in motion system installed on southbound roadway.

As shown in Fig. 6, conditioned signals from the sensor block are fed into an in-house built signal processing unit. A weather proof control box is fixed at the proximity of the bridge entrance and houses the signal processing unit including the signal conditioners, loop detectors, A/D converter, on-site processor unit, storage block, power management block, and two marine batteries that are charged through a solar panel.

3.2. Data acquisition system

The long-term monitoring system uses six data loggers *model 8020 manufactured by Geokon Inc.* that are placed at different locations along the bridge and were programmed to collect data from all sensors simultaneously with a *sampling time interval* of 20 min since time of construction to date. *Each datalogger is capable of acquiring data from vibrating wire sensors, Carlson type sensors, thermistors, thermocouples, Sonic probes, TDR cables, and all voltage type devices. One data logger can accommodate up to twelve single ended sensors for direct measurements, while this capacity can be expanded up to 256 channels by connecting eight multiplexers each with 32 channel capacity. The standard memory storage capacity in each datalogger is 62,000 data points, and can be expanded optionally to 1,000,000 data points. A digital signal processing unit (DSP) is incorporated with the datalogger to eliminate effects of electrical noise and interference on vibrating wire sensors.* The data loggers are placed in weather proof enclosures that are secured to the parapet wall and are accessible from the bridge side walk for maintenance purposes and/or for direct manual downloading of data. Vibrating wire sensors are wired to 28 multiplexers *model 8032* that are mounted at different locations along the full length of the bridge, each with 32 channel capacity. Each multiplexer communicates to the closest data logger through one single communication cable. All data loggers are daisy-chained together and can be accessed from the field office on a single coaxial cable. The communication cable is mounted on the parapet wall and runs along the bridge in a protective PVC conduit. The data acquisition system is equipped with a phone modem that enables remote monitoring and downloading of data from any location via a telephone line. Fig. 7 illustrates the configuration of data acquisition and distribution of logging units. All equipment, sensors, and data acquisition systems are powered through 12 V DC marine batteries that are continuously charged through photovoltaic solar panels. Each solar panel is mounted to a fifteen feet long stainless steel mast fixed to the bridge parapet wall at the location of the data loggers, as illustrated in Fig. 7. The marine batteries are housed in separate weather-proof enclosures in order to be isolated from the data loggers in an effort to secure the latter from any possible leakage of acid vapors.

4. Steel superstructure straining actions

In order to improve our understanding of long-term bridge performance, loading as well as response data need to be documented. This data will serve as a reference to the current methods of bridge design and construction, and could be used in the future to demonstrate advantages and disadvantages of different practices in bridge engineering. Fig. 8 shows the maximum positive and negative bending moment values measured on the steel girders. Fig. 9 shows a sample of axial forces developed on the steel girders, while Fig. 10 shows an example of shearing stresses. The bending moments (BM) and axial forces (AF) are calculated according to the following relations:

$$BM = \frac{I}{d}(\sigma_b - \sigma_t) \tag{1}$$

$$AF = \frac{A}{2}(\sigma_b + \sigma_t) \tag{2}$$

where I is the moment of inertia of the steel girders, d is the depth of the steel girders between top and bottom measurements and A is the steel beams cross-sectional area. σ_b and σ_t are stresses on the top and bottom of the steel girders, respectively, and can be calculated from the strain measurement at each location according to the relation:

$$\sigma = E(\varepsilon - \alpha \Delta T) \tag{3}$$

where E is the modulus of elasticity of the steel girder, ε is the measured strain value, α is the coefficient of thermal expansion of the steel material, and ΔT is the measured temperature change.

Shearing stresses (τ) are calculated as:

$$\tau = \gamma \times G \tag{4}$$

where G is the shear modulus of the steel girder material, and γ is shear strain measured using the 45° strain rosette according to:

$$\gamma = 2\varepsilon_2 - (\varepsilon_1 + \varepsilon_3) \tag{5}$$

where ε_1, ε_2, and ε_3 correspond to strain gages oriented at angles measuring 0°, 45°, and 90° with the horizontal plane respectively.

The bending moments' plots and shearing stresses show a close correlation between the measured values and those calculated theoretically due to the deck pours. The time history of the

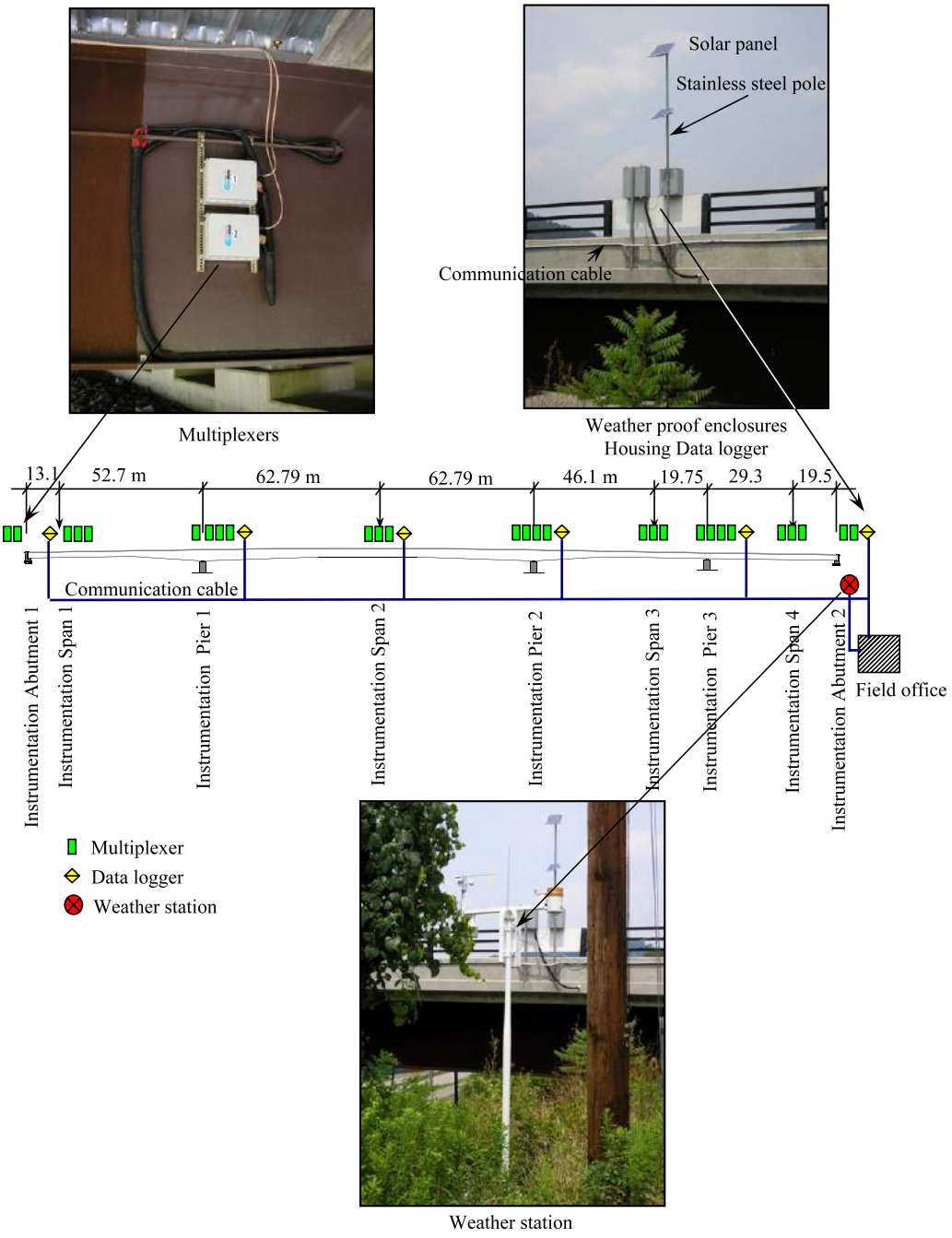

Fig. 7. Data acquisition system on Star City Bridge.

straining actions indicates that the governing loading condition in the superstructure is the dead weight of the concrete deck. The variation of bending moments in the steel superstructure due to seasonal environmental loading accounted for an average of 20 % of the dead weight value. It is worth mentioning here that the strain gages *have a response time for excitation and recording operation of* 1/2 *s, therefore* the dynamic effect of traffic loading is not included. After completion of the pouring sequence, the shearing stresses show little variation. Transverse cracks along the length of the concrete deck occurred shortly after the pouring sequence which would have released the internally built-in stresses. The bearings degrees of freedom allowed the steel superstructure to release the longitudinal stresses in the steel girders between Pier 2 and Abutment 2. This observation is confirmed by studying the expansion and contraction of the bridge ends relative to the abutment walls. Fig. 11 demonstrates the time history of the bridge expansion joint at both abutments. The design movement ratings indicate 30.48 cm at each abutment, for a minimum and maximum temperature range of −34 to 49 °C respectively. The average maximum and minimum deck temperature recorded over 4 years period is −14 and 40 °C respectively, which makes a range of 54 °C. The bearing design configuration assumes that the girders are fully pinned at Pier 2 and free to deform in the longitudinal direction at both abutments as well as at Pier 1 and Pier 3. The overall length of the bridge segment from Pier 2 till Abutment 1 measures 191.4 m, while the total length from Pier 2 till Abutment 2 is 114.6 m. Neglecting live load rotation and deflection at Pier #2, the range of movement at Abutments 1 and 2 are theoretically calculated to be 12.09 cm and 7.24 cm respectively. Compared to the actual field records, the range of motion at Abutment 2 is measured to be 7.34 cm, which is very close to the theoretically calculated one,

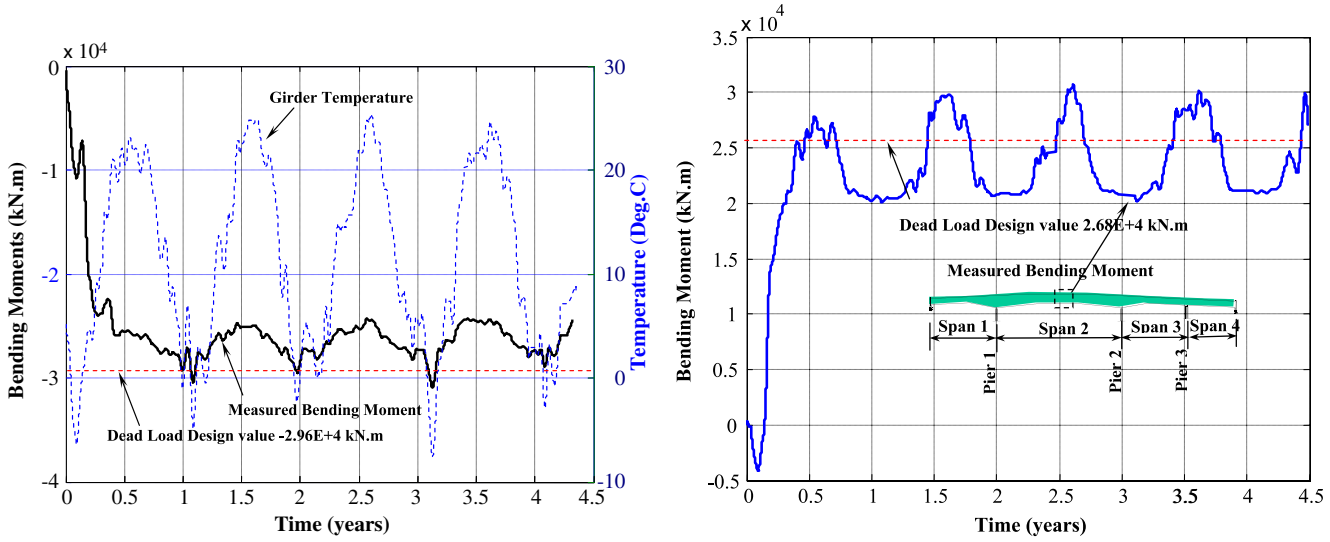

(a) Bending moment at Pier 1.

(b) Bending moment at Span 2.

Fig. 8. Time history of bending moments on Girder 7.

Table 2
Expansion and contraction range of bridge ends.

Location	Distance from Pier 2 (m)	Theoretical motion range (cm)	Measured motion (cm)
Abutment 1	191.4	12.09	5.91
Abutment 2	114.6	7.24	7.34

while the motion at Abutment 1 amounts to 5.91 cm which is about half of the theoretical value.

Table 2 summarizes the comparison between theoretically calculated and measured motion of the bridge ends at each abutment. The current design procedures assume that all axial stresses in the bridge superstructure are relieved by the expansion and contraction allowed by end bearings or by integral abutments action. The effect of end bearings constrains on the development of internal stresses in continuous steel girders has been overlooked in the literature and design procedures. Zhao and De Wolf [41] applied dynamic testing techniques to identify the overall changes in the structural behavior of a bridge and concluded that partial restrains in end bearings accounted for a change in the natural frequency of 15.4%. In this study, the partial movement restrains recorded at Abutment 1 explains the large axial forces developed at the steel girders, as shown in Fig. 8. The normal forces were developed since early age of construction and have not been released to date. Such internal stresses warrant to be taken into consideration in future design procedures.

5. Temperature loading

When designing for potential thermal effects, bridge designers have to take into consideration extreme thermal loading conditions that are likely to occur within the service life of the structure that may span over 50 years in most cases. Temperature measurements from the instrumentation system placed in the bridge superstructure were used to identify the range of temperature variations and provide an array of temperature profiles that can be used in the design of similar lightweight bridge superstructures.

In order to analyze temperature data, daily maximum and minimum temperatures are identified, as well as daily temperature gradients. As data are collected with an interval of 20 min, a computer program breaks the time history of collected temperature data into sequences of 24 h period spans (one day sequence), then identifies the maximum and minimum values of temperature from all

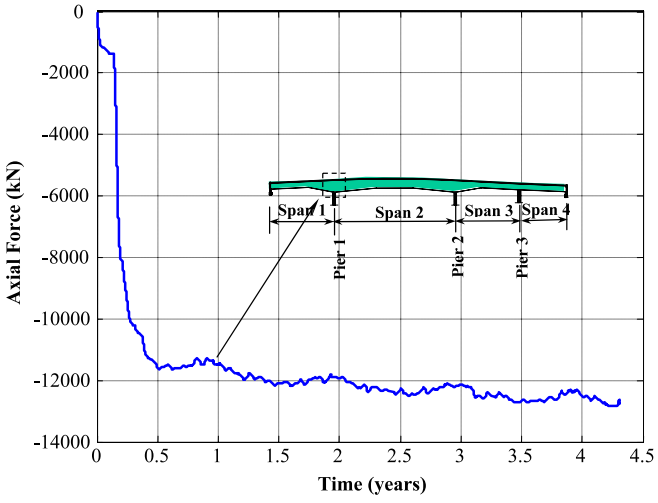

Fig. 9. Axial force on Girder 7 at Pier 1.

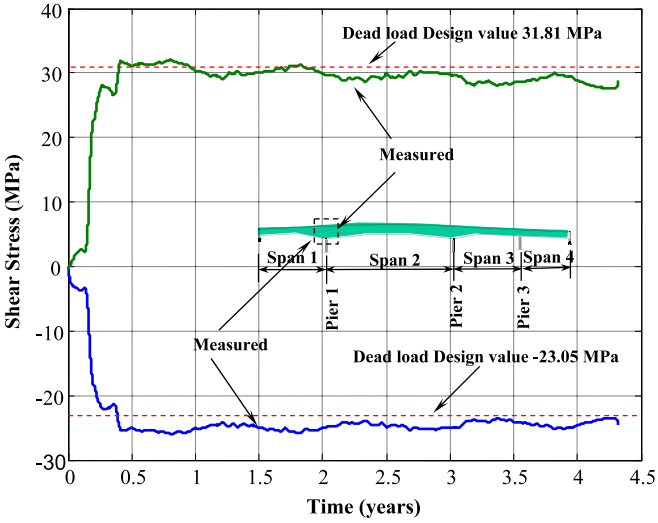

Fig. 10. Shear stresses on Girder 7 at Pier 1 towards span 1.

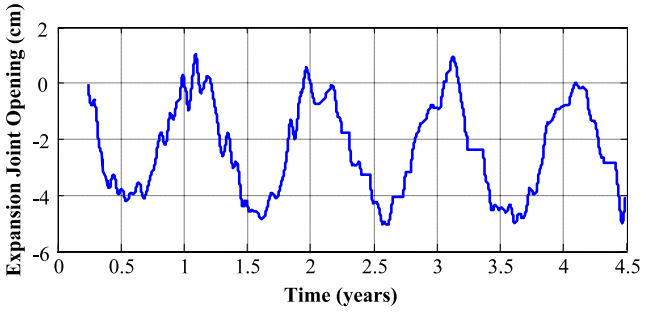

(a) Expansion joint at Abutment No. 1.

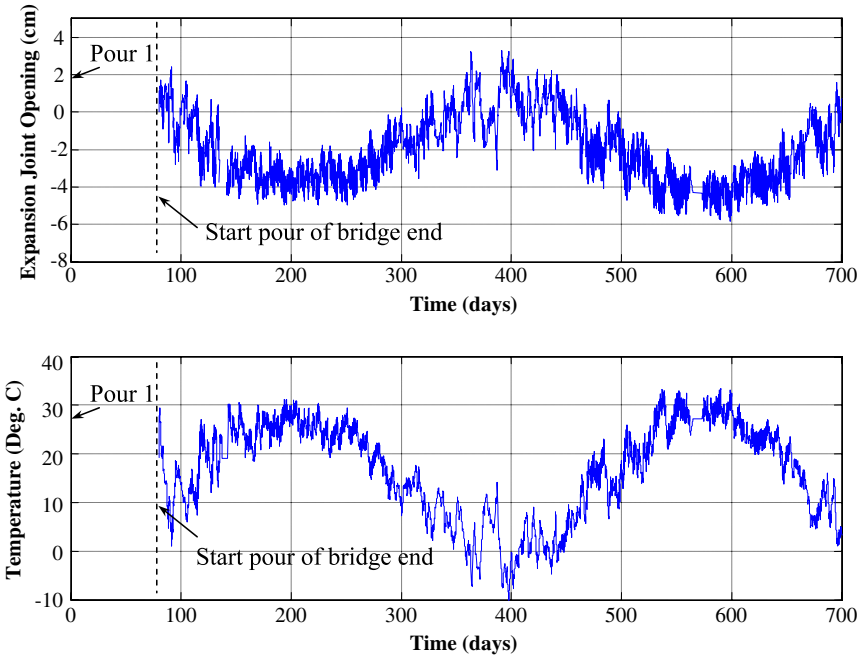

(b) Detailed Expansion joint at Abutment No. 2.

Fig. 11. Expansion joint openings.

thermistors in each day. The program also identifies temperature gradients across both the concrete deck thickness, as well as across the depth of the steel girders between measurement points at each day. The program then compares the maximum and minimum values of each day, as well as the positive and negative gradients, and identifies the greatest value and its location within the time history.

Table 3 summarizes the instantaneous absolute maximum positive temperature gradients identified from the temperature records along the bridge superstructure. The positive gradient indicates that the top fibers of the concrete deck measure warmer temperatures relative to the bottom fibers in the steel girders. In contrast, Table 4 summarizes the instantaneous absolute maximum negative temperature gradient in the bridge superstructure. The dates where maximum positive and negative gradients are identified to be 538 days and 364 days after placing the first concrete pour respectively. The maximum instantaneous positive temperature gradient is calculated from Table 3 to be 13.51 °C, while the instantaneous maximum negative gradient is calculated from Table 4 to be −11.38 °C. It is important to note here that such values are expected to increase if measured at the very top fibers of concrete deck, as well as the bottom fibers of steel girders.

Measured maximum positive and negative temperature gradients were compared with AASHTO LRFD Design gradients as shown in Fig. 12. The measured positive gradient is fairly close to that within the AASHTO gradient, while the measured negative differential through the deck is found higher than that of the AASHTO.

Analysis of temperature across the bridge width also indicates that a temperature gradient exist in the transverse direction.

Table 3
Maximum positive temperature gradient in bridge superstructure.

Location	Top Temp. (°C)	Bottom Temp. (°C)	Gradient
Mid-span 4	38.55	27.77	10.78
Pier 3	38.39	27.51	10.88
Mid-span 3	39.83	26.61	13.22
Pier 2	34.75	23.56	11.19
Mid-span 2	36.47	22.96	13.51
Pier 1	35.64	23.5	12.14
Mid-span 1	38.55	26.02	12.53

Table 4
Maximum negative temperature gradient in bridge superstructure.

Location	Top Temp. (°C)	Bottom Temp. (°C)	Gradient
Mid-span 4	−8.28	2.89	−11.16
Pier 3	−7.8	3.57	−11.38
Mid-span 3	−7.86	2.71	−10.58
Pier 2	−7.43	2.46	−9.88
Mid-span 2	−7.07	3.33	−10.41
Pier 1	−7.34	3.44	−10.78
Mid-span 1	−8.22	2.15	−10.37

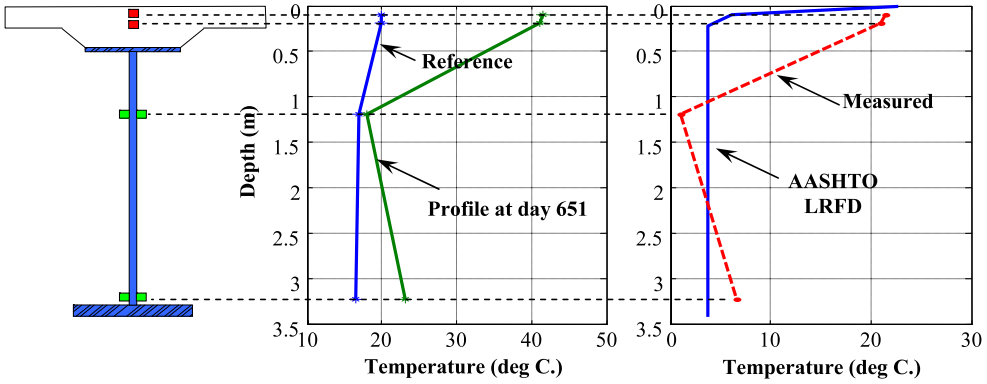

(a) Positive temperature gradient.

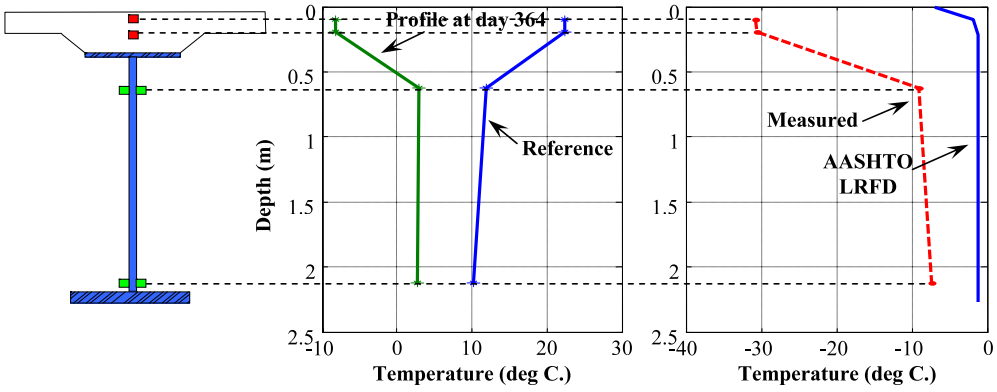

(b) Negative temperature gradient.

Fig. 12. AASHTO LRFD, and Measured Temperature Gradients.

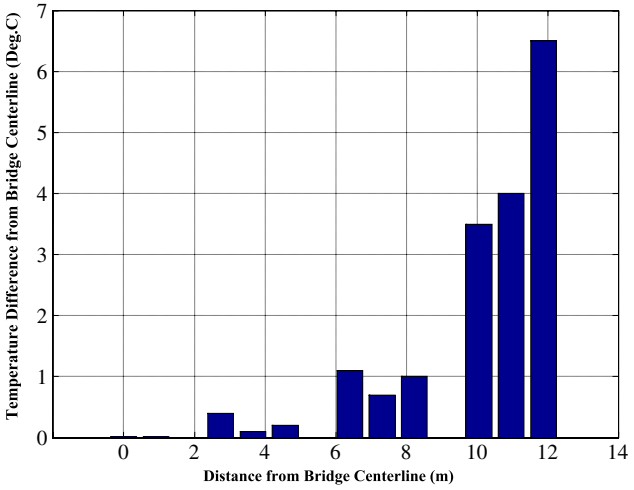

Fig. 13. Temperature gradient across bridge width at day 294.

Measurement of the temperature at the diaphragm members on Abutment 2 have been used to evaluate the temperature gradient across the bridge width. Taking the reference temperature to be that at the centerline of the bridge, Fig. 13 illustrates the difference in temperature values across the bridge width. It can be noticed that a non-uniform gradient of values up to 6.5 °C (11.7 °F) occurs across the bridge. Consequently, this environmental loading configuration is expected to add internal stresses in the superstructure, especially at the transverse direction in elements such as diaphragm members, as well as the concrete deck.

Axial forces and bending moments of the instrumented diaphragm members are calculated based on linear thermo-elastic approach. With the exception of a small number of members, the straining actions in diaphragms seem to be more affected by temperature variations. A comparison between design calculations and measured values could be carried out at the location of the abutments. A comparison of the maximum measured compression axial forces at the diagonal members and those factored values from design calculation sheets is shown in Fig. 14.

The axial forces in each member is calculated through the thermo-elastic relation:

$$F = (\varepsilon - \alpha \Delta T) \times E \times A_{diaph} \tag{6}$$

where: F = Axial force in diaphragm member
E = Modulus of elasticity of the steel.
ε = measured axial strain.
ΔT = measured temperature change.
α = Coefficient of thermal expansion of steel.
A_{diaph} = Cross sectional area of diaphragm member.

As illustrated in Fig. 14, the axial forces in the interior inclined members are fairly close to those calculated theoretically. However, the forces within the outer members show a gradual increase and reach their maximum values between Girder No. 7 and Girder No. 8. Intuitively, the bridge's edge girder (Girder No. 8) is more subjected to solar radiation, and more susceptible to large deformations rather than the bridge center, by virtue of its location. Thus, the bracing members located towards the bridge side would be subjected to more excessive stresses than those towards the bridge center. To demonstrate the effect of the temperature gradient across the bridge width, a comparison between designed stresses and measured ones on the outside diaphragm member is

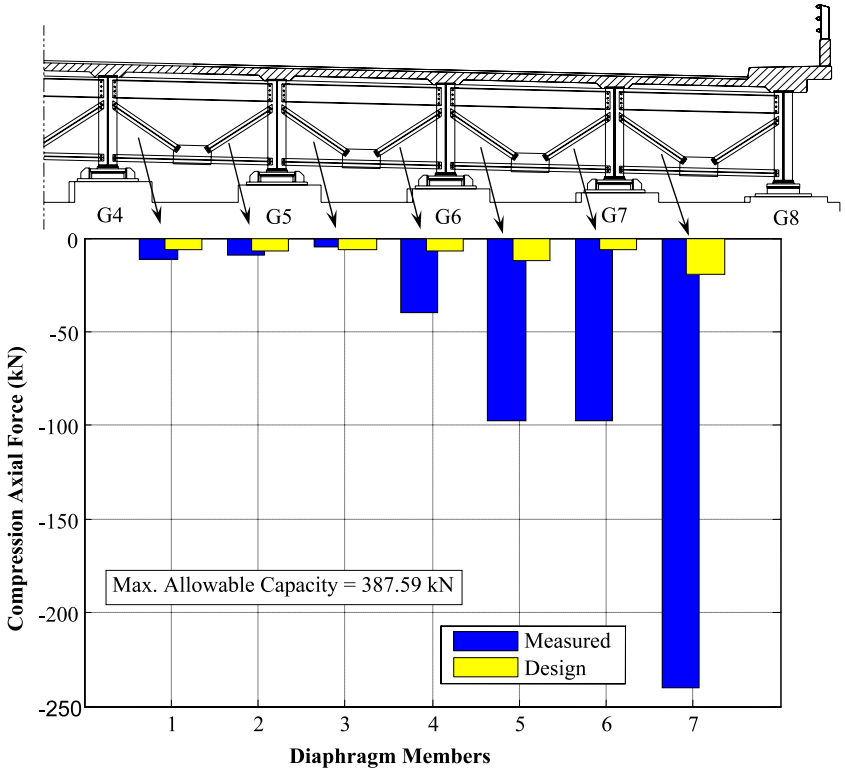

Fig. 14. Maximum axial compression force in bracing members at Abutment 2.

conducted. The maximum allowable capacity in compression of the inclined diaphragm members from design calculation sheets is 387.59 kN (87.14 kips). The maximum compression value of the diagonal diaphragm member at this location was measured to be 240.2 kN (54 kips), which is 62% of the members' maximum capacity. This comparison indicates that the outside diaphragm members are not behaving as secondary structural members anymore.

6. Conclusions

This paper demonstrates the instrumentation system implemented on the Star City Bridge in West Virginia for long-term structural monitoring of a lightweight bridge superstructure. The instrumentation system is successful to secure long-term records of bridge data such as strains in the concrete deck, stresses and straining actions in the steel superstructure, expansion and contraction of the deck, temperature gradients and environmental loading configurations, along with traffic data. Analysis of the state of stresses in the steel girders indicate that the primary loading factor is the deck's own weight, while temperature and environmental effects had up to 20% impact on the variation in girders stresses once deck cracks occur. Measurement of the expansion and contraction of one bridge end relative to the abutment wall was found to be very close to that calculated theoretically, which contributed to the relief of built-in girder stresses in the longitudinal direction in this segment. Bearing constrains on the other bridge end induced large compression forces on the steel girders. Analysis of temperature data demonstrates a non-uniform temperature gradient across the bridge width with magnitudes up to 6.5 °C. This temperature gradient is not accounted for in any design procedures and has a direct impact on the stresses in the diaphragm members. The maximum measured positive gradient through the superstructure depth is within the specifications of the AASHTO LRFD, while the measured negative differential through the deck was found to have a higher value.

Acknowledgments

The authors wish to acknowledge the West Virginia Department of Transportation for sponsoring this research program and for their active support throughout the various phases of construction and sensor installations. The authors gratefully appreciate the cooperation and support of all engineers and officials in District four and WVDOH and in particular Engineering Division and Materials Division.

References

[1] (AASHTO) American Association of State Highway and Transportation Officials (2008) Bridging the Gap. July 2008.
[2] Chase Steven B. Long term bridge monitoring to support bridge technology innovations,. In: 19th US-Japan bridge engineering workshop; 2003.
[3] Frangopol DM, Kong JS, Gharaibeh ES. Reliability based life-cycle management of highway bridges. J. Comput. Civ. Eng., ASCE 2001;15(1):27–34.
[4] Chase StevenB. The role of sensing and measurement in achieving FHWA's strategic vision for highway infrastructure. In: Sensing issues in civil structural health monitoring. Springer; 2005. p. 23–32.
[5] Aktan AE, Helmicki AJ, Hunt VJ, Levi A. Instrumentation, testing, and monitoring of a newly constructed reinforced concrete deck-on-steel girder bridge—Phases I and II. Report No. FHWA/OH-99/013, Ohio Department of Transportation, (Columbus, OH); 1999.
[6] Mufti AA, Bakht B, Tadros G. SHM technologies for civil engineering intelligent infrastructure. In: Structural health monitoring and intelligent infrastructure. London: Taylor and Francis Group; 2006.
[7] Aktan AE, Catbas FN, Grimmelsman K, Pervizpour M, Curtis J, Shen K, Quin X. SPIE 2002;4696:17–29.
[8] Lenett MS, Hunt VJ, Helmicki AJ, Aktan AE. Instrumentation, testing and monitoring of a newly constructed reinforced concrete deck-on-steel girder bridge — Phase III. Report No. UC-CII 01/1. Cincinnati Infrastructure Institute, University of Cincinnati, Ohio; 2001.
[9] Catbas FN, Shah M, Burkett J, Basharat A. Challenges in structural health monitoring, In: 4th international workshop on structural control; 2004.
[10] Nassif H, Gucunski N, Abu-amra T, Gindy M, Balic M. Analytical modeling and instrumentation planning of the Doremus Avenue Bridge. Final Report FHWA-NJ-2002-008, New Jersey Department of Transportation. (Trenton, NJ); 2002.
[11] Rizkalla S, Benmokrane B, Tadros G. Structural health monitoring bridges with fibre optic sensors. In: European COST F3 conference on system identification and structural health monitoring. 2000. pp. 501–510.

[12] William GW, Shoukry SN, Riad MY. Thermal stresses in steel girder bridges with integral abutments. J. Bridge Struct. 2005;1(2):103–19.
[13] Strauss A, Frangopol DM, Kim S. Use of monitoring extreme data for the performance prediction of structures: Bayesian updating. J. Eng. Struct. 2008; 30(12):3654–66. Available online at: http://www.sciencedirect.com/science/journal/01410296.
[14] DeWolf JT, Conn PE, O'Leary PN. Continuous monitoring of bridge structures. In: IABSE symp., int. association for bridge and structural engineering; 1995.
[15] Nagayama T, Abe M, Fujino Y, Ikeda K. Structural identification of non-proportional damped systems and its applications to a full scale suspension bridge. J. Struct. Eng., ASCE 2005;131(10):1536–45.
[16] Ren W, Harik I, Blandford G, Lenett M, Baseheart T. Roebling suspension bridge. II: Ambient testing anf live load response. J. Bridge Eng., ASCE 2004;119–26.
[17] Raghavendrachar M, Aktan AE. Flexibility by multireference impact testing for bridge diagnostics. J. Struct. Eng. 1992;118(8):2186–203.
[18] Aktan AE, Lee L, Dalal V. Multireference modal testing for bridge diagnostics, North American workshop on instrumentation and vibration analysis of highway bridges; 1995.
[19] Toksoy T, Aktan AE. Bridge-condition assessment by modal flexibility, In: Proceeding, North American workshop on instrumentation and vibration analysis of highway bridges; 1995.
[20] Alampalli S, Fu G, Dillon EW. Measuring bridge vibration for detection of structural damage. Report no. FHWA/RR-95/165; 1995.
[21] Sohn H, Farrar CR, Hunter NF, Worden K. Structural health monitoring using statistical pattern recognition techniques. ASME J. Dynam. Syst. Meas. Control: Special Issue on Identification of Mechanical Systems 2001;123(4):706–11.
[22] AASHTO LRFD bridge design specifications. 2nd ed. American Association of State Highway and Transportation Officials. (Washington, D.C.); 1998.
[23] AASHTO LRFD bridge design specifications. 2nd ed. American Association of State Highway and Transportation Officials. (Washington, D.C.); 2004.
[24] AASHTO LRFD bridge design specifications. 4th ed. American Association of State Highway and Transportation Officials. (Washington, D.C.); 2007.
[25] Maser K, Egri R, Lichtenstein A, Chase S. Field evaluation of a wireless global bridge evaluation and monitoring system. In: Proceeding, 11th conf. on engineering mechanics. Vol. 2. Fort Lauderdale. (Fla). 1996. pp. 955–958.
[26] Straser EG, Kiremidjian AS. A modular wireless damage monitoring system for structures. Report no. 128. John A. Blume Earthquake Engineering Center. (Stanford, CA); 1998.
[27] Bennett R, Hayes-Gill B, Crowe JA, Armitage R, Rodgers D, Hendroff A. Wireless monitoring of highways, smart systems for bridges, structures and highways, Newport Beach, CA. Proc. SPIE 1999;3671:173–82.
[28] Lynch JP. Decentralization of wireless monitoring and control technologies for smart civil structures. Report no. 140. John A. Blume Earthquake Engineering Center. (Stanford, CA); 2002.
[29] Lynch JP, Sundararajan A, Law KH, Sohn H, Farrar CR. Design of a wireless active sensing unit for structural health monitoring. In: Proceedings of the 11th annual international symposium on smart structures and materials; 2004.
[30] Mitchell K, Rao VS, Pottinger HJ. Lessons learned about wireless technologies for data acquisition, smart structures and materials, CA. Proc. SPIE 2002;4334: 234–43.
[31] Kottopalli VA, Kiremidjian AS, Lunch JP, Carryer E, Kenny TW, Law KH, Lei Y. Two-tiered wireless sensor network architecture for structural health monitoring, smart structures and materials, CA. Proc. SPIE 2003;5057:8–19.
[32] Mastroleon L, Kiremidjiana AS, Carryerb E, Law KH. Design of a new power-efficient wireless sensor system for structural health monitoring. Proc. SPIE 2004;5395:51–60.
[33] Lynch JP, Law KH, Kiremidjian AS, Carryer E, Farrar CR, Sohn H, Allen D, Nadler B, Wait J. Laboratory and field validation of a wireless sensing unit design for structural monitoring. In: Proceedings of US-Korea workshop on smart structural systems; 2002.
[34] Aoki S, Fujino Y, Abe M. Intelligent bridge maintenance systems using MEMS and network technology, smart systems and NDE for civil infrastructures, CA. Proc. SPIE 2003;5057:37–42.
[35] Shinozuka M, Feng MQ, Chou P, Chen Y, Park C. MEMS-based wireless real-time health monitoring of bridges. In: Proceeding of the 3rd international conference on earthquake engineering; 2004.
[36] Basheer MR, Rao V, Derriso M. Self-organizing wireless sensor networks for structural health monitoring. In: Proceeding 4th international workshop on structural health monitoring. 2003. pp. 1193–1206.
[37] Lynch JP, Wang Y, Law KH, Yi JH, Lee CG, Yun CB. Validation of a large-scale wireless structural monitoring system on the Geumdang Bridge. In: Proceeding, int. conf. on safety and structural reliability. 2005.
[38] Ruiz-Sandoval M, Nagayama T, Spencer BF. Sensor development using Berkeley Mote platform. J. Earthq. Eng. 2006;10(2):289–309.
[39] Pakzad SN, Fenves GL, Kim S, Culler DE. Design and implementation of scalable wireless sensor network for structural monitoring. J. Infrastruct. Syst., ASCE 2008;14(1):89–101.
[40] ASTM-E-1318. Standard specification for highway Weigh-in-Motion (WIM) systems with user requirements and test methods. American Society for Testing and Materials. 2002.
[41] Zhao J, DeWolf JT. Dynamic monitoring of steel girder highway bridge. J. Bridge Eng. 2002;7(6):350–6.